

The effect of grain size and grain orientation on deformation twinning in a Fe–22 wt.% Mn–0.6 wt.% C TWIP steel

I. Gutierrez-Urrutia*, S. Zaefferer, D. Raabe

Max-Planck-Institut für Eisenforschung, Max-Planck Str. 1, D-40237 Düsseldorf, Germany

ARTICLE INFO

Article history:

Received 14 December 2009

Received in revised form 10 February 2010

Accepted 11 February 2010

Keywords:

EBSD

Mechanical characterization

Steel

Twinning

ABSTRACT

We investigate the effect of grain size and grain orientation on deformation twinning in a Fe–22 wt.% Mn–0.6 wt.% C TWIP steel using microstructure observations by electron channeling contrast imaging (ECCI) and electron backscatter diffraction (EBSD). Samples with average grain sizes of 3 μm and 50 μm were deformed in tension at room temperature to different strains. The onset of twinning concurs in both materials with yielding which leads us to propose a Hall–Petch-type relation for the twinning stress using the same Hall–Petch constant for twinning as that for glide. The influence of grain orientation on the twinning stress is more complicated. At low strain, a strong influence of grain orientation on deformation twinning is observed which fully complies with Schmid's law under the assumption that slip and twinning have equal critical resolved shear stresses. Deformation twinning occurs in grains oriented close to $\langle 111 \rangle$ /tensile axis directions where the twinning stress is larger than the slip stress. At high strains (0.3 logarithmic strain), a strong deviation from Schmid's law is observed. Deformation twins are now also observed in grains unfavourably oriented for twinning according to Schmid's law. We explain this deviation in terms of local grain-scale stress variations. The local stress state controlling deformation twinning is modified by local stress concentrations at grain boundaries originating, for instance, from incoming bundles of deformation twins in neighboring grains.

© 2010 Elsevier B.V. All rights reserved.

1. Introduction

TWIP (twinning-induced plasticity) steels have received high interest in recent years due to their outstanding mechanical properties at room temperature combining high strength (ultimate tensile strength of up to 800 MPa) and ductility (elongation to failure up to 100%) based on a high work-hardening capacity [1–3]. TWIP steels are austenitic steels, i.e. face-centered cubic (fcc) metals, with high content in Mn (above 20% in weight %) and small additions of elements such C (<1 wt.%), Si (<3 wt.%), or Al (<3 wt.%). The steels have low stacking fault energy (between 20 and 40 mJ/m² [3–5]) at room temperature. Although the details of the mechanisms controlling strain-hardening in TWIP steels are still unclear, the high strain-hardening is commonly attributed to the reduction of the dislocation mean free path with the increasing fraction of deformation twins as these are considered to be strong obstacles to dislocation glide [3,6–8]. Therefore, a quantitative study of deformation twinning in TWIP steels is critical to understand their strain-hardening mechanisms and mechanical properties. Deformation twinning can be considered as a nucleation and growth process [9]. Twin growth is assumed to proceed by co-operative

movement of Shockley partials on subsequent $\{111\}$ planes. Possible mechanisms for the co-operative movement are the pole mechanism [10], a cross-slip mechanism [11] or the reaction between primary and secondary slip systems [12,13]. Nucleation of deformation twins, on the other hand, consists in the formation of the dislocation structures required for twin growth and a number of experimental observations suggest mechanisms for that [9,14,15]. Dislocation slip is therefore a prerequisite for twin formation. The stress required to produce twins in a microstructure, generally termed as twinning stress, is a mixture of the stress for twin nucleation and that for growth. However, as the experimental determination of the stress needed for twin nucleation is very difficult to accomplish [9], it is commonly assumed that the twin nuclei already exist and, hence, only the stress for twin growth can be experimentally measured which is generally identified as the twinning stress. As the growth of a deformation twin is controlled by the glide of Shockley partials, it is reasonable to assign a critical resolved shear stress on the slip plane to this process that must be reached to move the twinning dislocations leading to the deformation twinning. For the same material in an undeformed state, the main parameters that may influence the twinning stress and, hence, the twinning microstructure, are grain size and grain orientation. Only few studies have addressed the influence of these microstructural parameters on deformation twinning in TWIP steels [5,16,17]. Ueji et al. [5] reported a strong

* Corresponding author. Tel.: +49 2116792 211.

E-mail address: i.gutierrez@mpie.de (I. Gutierrez-Urrutia).

influence of grain size on deformation twinning in a Fe–31 wt.% Mn–3.0 wt.% Al–3.0 wt.% Si TWIP steel. They observed that deformation twinning is strongly inhibited for an average grain size of 1.8 μm suggesting that deformation twinning in TWIP steels becomes difficult as the grain size decreases to a certain scale. Yang et al. [16] and Meng et al. [17] reported a strong influence of grain orientation on twinning behavior in a Fe–33 wt.% Mn–3.0 wt.% Al–3.0 wt.% Si TWIP steel. They found that deformation twinning is favored during tension because the grains rotate towards the $(1\ 1\ 1)$ /tensile axis which renders the crystals favorably oriented for twinning (high Schmid factor) whereas deformation twinning is suppressed during compression because the grains rotate towards the $(1\ 0\ 1)$ axis which renders them unfavorably oriented for twinning (small Schmid factor). However, there are still some details that remain unclear regarding the influence of grain size and grain orientation on twinning behaviour in TWIP steels, in particular their role on the twinning stress. The aim of this report is to investigate in detail the influence of grain size and grain orientation on the twinning behavior in a Fe–22 wt.% Mn–0.6 wt.% C TWIP steel. Detailed microstructural observations by electron channeling contrast imaging (ECCI) and electron backscatter diffraction (EBSD) were performed on tensile deformed samples at room temperature to different strains with average grain sizes of 3 μm and 50 μm . Further analyses based on stress–strain curves and deformed microstructures were carried out to illustrate the effect of grain size and grain orientation on the twinning stress.

2. Experimental details

The TWIP steel used in this study had the chemical composition Fe–22 wt.% Mn–0.6 wt.% C. The material was melted in an induction furnace under Ar atmosphere and cast to round bars of 25 mm diameter. To avoid Mn segregation [18] samples were swaged to 20% area reduction at 1000 °C and subsequently solution-treated for 4 h at 1100 °C under Ar. Thereafter, samples were hot-rolled to 75% reduction in thickness at 1000 °C followed by air cooling. The hot-rolled material was then cold rolled to 70% thickness reduction. In order to obtain different grain sizes, the material was finally annealed at 700 °C for 5 or 15 min resulting in material with average grain size of 3 μm (referred to as steel FG) and 50 μm (referred to as steel LG), respectively. Tensile tests were carried out at room temperature at a strain rate of $5 \times 10^{-4} \text{ s}^{-1}$ to different strains. The tensile bone-shaped samples had 8 mm gage length, 2 mm gage width and 1 mm gage thickness. The monotonic tensile deformation experiments were carried out on a tensile test instrument Kammrath & Weiss GmbH (44141 Dortmund, Germany) equipped with a digital image correlation (DIC) system (ARAMIS system, GOM-Gesellschaft für Optische Messtechnik mbH, 38106 Braunschweig, Germany) to measure the local and macroscopic strain distribution. Details of this setup are described in [19–22]. The surface pattern required for DIC was obtained by applying two different colour sprays on the sample surface. Firstly, a white spray was used to obtain a homogeneous background and thereafter, a black spray was applied to obtain a spotted pattern. Averaged engineering strain values are obtained from the corresponding maps and utilized to calculate the logarithmic stress–strain values.

Deformation microstructures of the tensile deformed TWIP steels were examined by two scanning electron microscopy techniques: electron back scatter diffraction (EBSD) and electron channeling contrast (ECCI). The EBSD technique was used to analyze the local texture in relation with the microstructure. Orientation maps were performed in a 6500 F JEOL field emission gun-scanning electron microscope (FEG-SEM) equipped with a TSL

OIM EBSD system. EBSD maps were measured at 15 kV acceleration voltage and a working distance of 15 mm. The ECCI technique has been recently proven as a powerful technique to image deformation twins and even dislocation structures in TWIP steels by using a SEM [23]. A new recently reported setup for ECCI [23] was used in this study to obtain ECCI images under controlled diffraction conditions with enhanced dislocation and interface contrast. ECCI observations were carried out in a Zeiss Crossbeam instrument (XB 1540, Carl Zeiss SMT AG, Germany) consisting of a Gemini-type field emission gun (FEG) electron column and an focused ion beam (FIB) device (Orsay Physics). ECCI was performed at 10 kV acceleration voltage and a working distance of 6 mm, using a solid-state 4-quadrant BSE detector. The microscope was run in the “high current” mode and an objective lens aperture of 120 μm was used.

3. Results

3.1. Effect of grain size

The initial hot-rolled state of both materials (LG and FG) showed a fully austenitic structure which remained stable during deformation. No evidence of ϵ -martensite was detected by EBSD. The initial hot-rolled textures on both materials were weak, and during tensile deformation both steels developed similar deformation textures which are shown below. The similarity of deformation textures allows us to analyze the influence of grain size on deformation twinning by examining the deformation microstructures in samples LG and FG at similar strain levels.

The ECCI technique was found to be an excellent tool in examining deformation microstructures of TWIP steels. The onset of deformation twinning in steel LG was observed at a logarithmic strain of 0.03. At this strain level the twin fraction was very small (twin area fraction less than 0.001 determined from ECCI pictures of around 100 grains) and only few grains, less than 20%, contained deformation twins. In most of these grains only one twinning system (primary system) was activated. Fig. 1(a) shows an ECCI image of the microstructure of steel LG tensile deformed to 0.03 logarithmic strain. Grains containing deformation twins up to 50 μm in length and 0.5 μm in thickness, which are nucleated at grain boundaries, are visible. This ECCI image was obtained by orienting the grain in the centre of the image into Bragg condition for the diffraction vector $g: (1\ \bar{1}\ 1)$. Under this diffraction condition, details of deformed microstructure such as deformation twins, orientation gradients (grey areas), and even dislocation structures can be identified at optimum contrast. At higher magnification it is further observed that deformation twins are not single but bundles consisting of thinner twins, as shown in Fig. 1(b). For this ECCI image optimum contrast was achieved by tilting the sample such as to excite the $(0\ 0\ 2)$ diffraction vector of the twins in a “two-beams” condition. It is observed that the bundle, around 0.5 μm thick, consists of six thin twins (dark straight lines) with thickness values ranging from 30 nm to 200 nm. Increasing the strain to a logarithmic strain of 0.3 lead to a significant increase in the twin area fraction from zero to around 0.2, Fig. 1(c). Almost all the grains contained deformation twins activated in several systems (up to three activated twinning systems were observed in the same grain) and only less than 10% of the grains contained no twins. The microstructure was very heterogeneous consisting of grains with only the primary twinning system activated, grains with more than one twinning system activated (primary and secondary twinning systems), and grains with no twins.

Deformation twins were also observed by ECCI in steel FG deformed to low strains. Fig. 2(a) shows an ECCI image of the microstructure of steel FG deformed to 0.04 logarithmic strain.

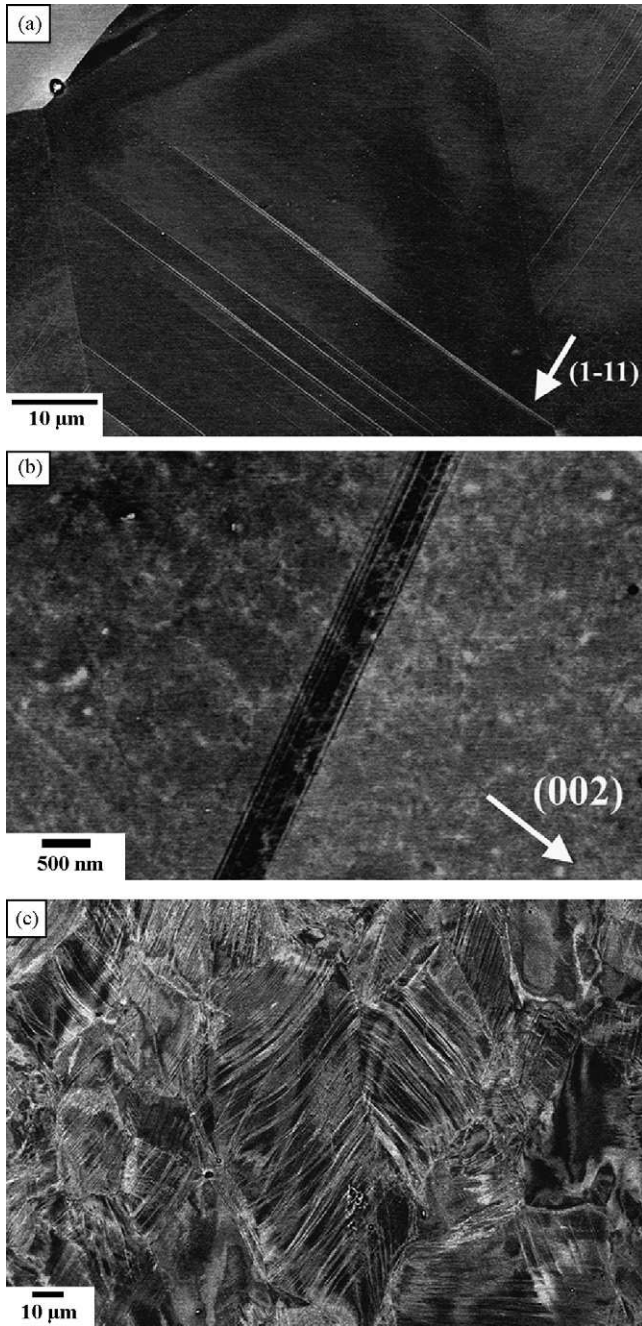


Fig. 1. Microstructures of steel LG (average grain size $50\ \mu\text{m}$) tensile deformed to 0.03 logarithmic strain (a and b) and 0.3 logarithmic strain (c). (a) ECCI image obtained in a SEM of grains containing bundles of deformation twins: diffraction vector $g: (1\ 1\ 1)_{\text{matrix}}$; (b) ECCI image of detail of a bundle containing thin twins (dark lines): diffraction vector $g: (0\ 0\ 2)_{\text{twin}}$.

Grains containing thin deformation twins (thickness 50–100 nm) are clearly observed, some of these twins are indicated with black arrows. Deformation twins were found even in grains smaller than $1\ \mu\text{m}$. Nevertheless, at this strain level the twin area fraction was very small, almost zero. At a higher logarithmic strain of 0.3 there was a significant increase in the twin area fraction, from zero to around 0.1. This increase in the twin area fraction is, however, smaller than in steel LG for the same strain level. Fig. 2(b) shows an ECCI image of the microstructure of steel FG strained to 0.3 logarithmic strain. The microstructure is very heterogeneous, like that observed for steel LG, containing grains with twins and grains with no twins. Most of the grains contained twins (around 80%) with

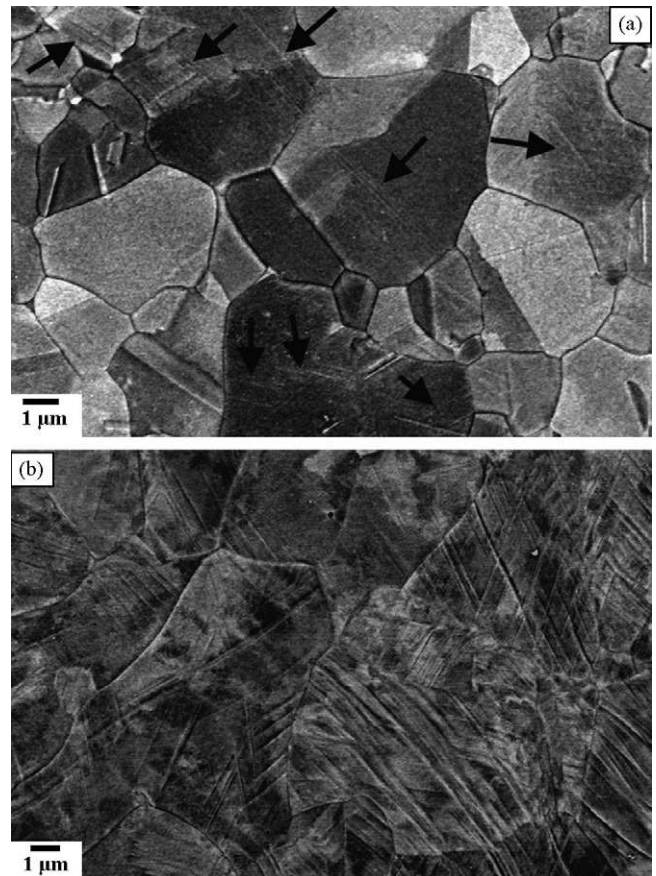


Fig. 2. ECCI images of microstructures containing deformation twins of steel FG (average grain size $3\ \mu\text{m}$), tensile deformed to 0.04 logarithmic strain (a) and 0.3 logarithmic strain (b). Black arrows indicate deformation twins.

different primary and secondary twinning systems activated.

3.2. Effect of grain orientation

We study the influence of grain orientation on deformation twinning during tensile deformation at room temperature on steel LG by means of EBSD. EBSD maps are displayed as image quality (IQ) maps and inverse pole figure (IPF) maps in the direction of tensile axis (TA). For better understanding of the influence of grain orientation on twinning, we analyze two deformation states: one at low strain (0.05 logarithmic strain) and another one at large strain (0.3 logarithmic strain).

Fig. 3(a) shows the inverse pole figure for the crystal direction along the tensile axis (TA-IPF) of the initial hot-rolled state indicating a weak texture of the starting state. Figs. 3(b) and (c) show TA-IPFs of the steel deformed to low and high strains, respectively. We observe that texture sharpens during tensile deformation, leading to texture components characterized by $\langle 111 \rangle // \text{TA}$ and $\langle 001 \rangle // \text{TA}$. Similar textures have been observed before in tensile deformed TWIP steels at room temperature [5,24]. Fig. 4 presents an example of an EBSD map performed on a sample strained to 0.05 logarithmic strain. As some twins are thinner than the resolution limit of the EBSD map, the TA-IPF map of Fig. 4(b) reveals a reduced number of indexed twins. However, in the image quality (IQ) map of Fig. 4(a) a higher number of twins is visible, appearing as straight thin dark lines. At this strain level, around one-third of the grains contained twins, mainly with only the primary twinning system activated. Fig. 5 shows a typical EBSD map performed on a sample strained to 0.3 logarithmic strain. At this strain level, bundles of twins were normally thicker than 100 nm and, therefore, most of

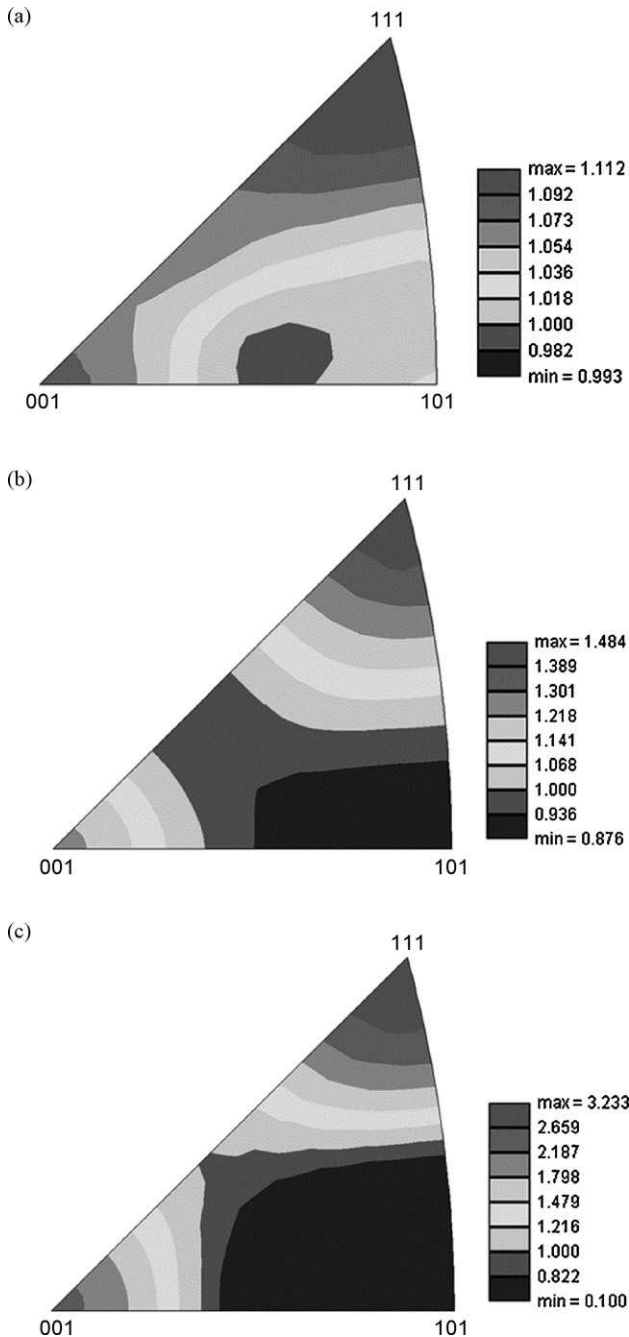


Fig. 3. Inverse pole figures along tensile axis direction of steel LG (average grain size 50 μm) at different states: as hot-rolled (a); tensile deformed to 0.03 logarithmic strain (b); tensile deformed to 0.3 logarithmic strain (c).

the twins can be indexed in the TA-IPF map. This figure shows that most of the grains, around 90%, contained deformation twins with several secondary activated twinning systems.

In order to study the influence of grain orientation on deformation twinning around 100 grains were analyzed in each deformation state. The orientation dependence of deformation twinning of steel LG to low strain and high strains is shown in Fig. 6(a) and (b), respectively. These TA-IPFs show orientations of grains containing twins (black dots) and of grains without twins (red dots). The TA-IPF of Fig. 6(a) shows that in the weakly strained LG sample there is a strong influence of the grain orientation on twinning activity. Deformation twinning mainly occurs in grains that are oriented close to the $\langle 111 \rangle // \text{TA}$ directions and only a small

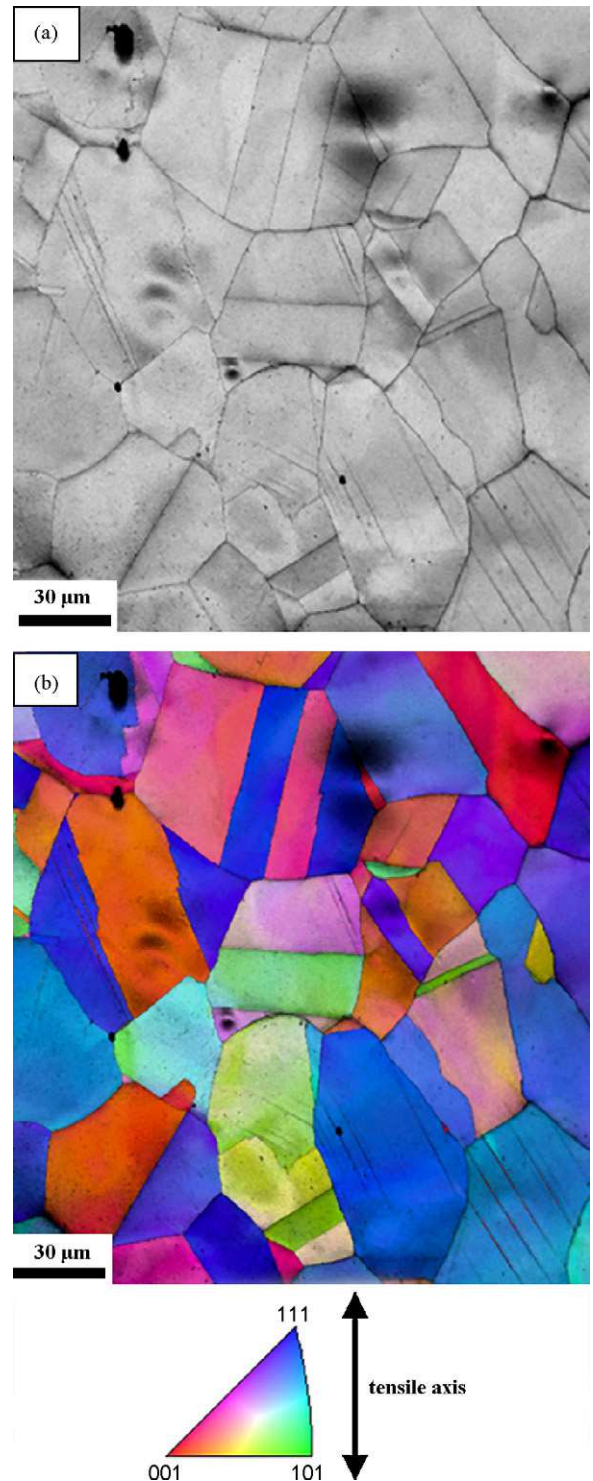


Fig. 4. EBSD map of steel LG (average grain size 50 μm) tensile deformed to 0.05 logarithmic strain. Diffraction pattern quality map (a), TA-IPF map (b) (TA: tensile axis; IPF: inverse pole figure).

fraction of grains with other orientations contain twins. Interestingly, at higher strain the influence of grain orientation on twinning activity decreased significantly. The TA-IPF given in Fig. 6(b) shows that in the highly strained LG sample, grains with almost all occurring orientations contained deformation twins and only grains oriented close to $\langle 001 \rangle // \text{TA}$ directions with angular deviation less than 5° contained no twins.

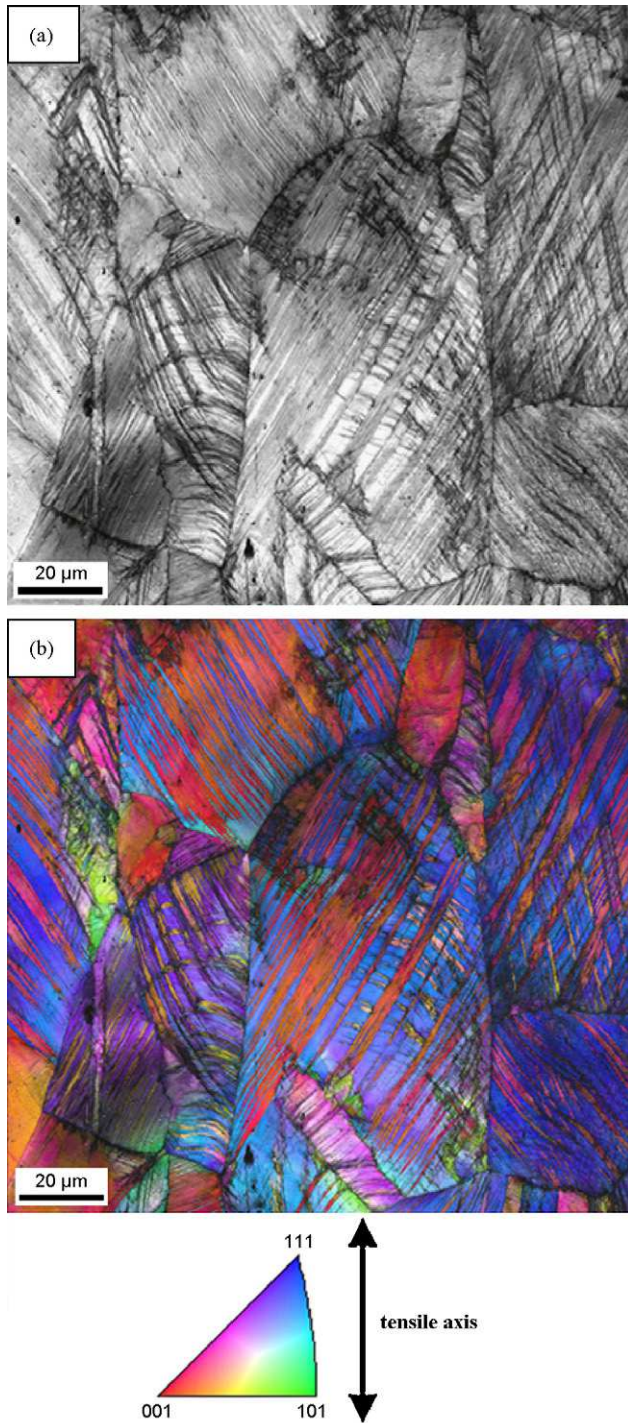


Fig. 5. EBSD map of steel LG (average grain size 50 μm) tensile deformed to 0.3 logarithmic strain. Diffraction pattern quality map (a), TA-IPF map (b) (TA: tensile axis; IPF: inverse pole figure).

4. Discussion

4.1. Effect of grain size

The main finding concerning the influence of grain size on deformation twinning is that grain refinement within the micrometer range does not suppress deformation twinning for the present TWIP steel tensile deformed at room temperature. Deformation twinning becomes more difficult as the average grain size decreases to 3 μm but it is not completely suppressed. Grain refinement pro-

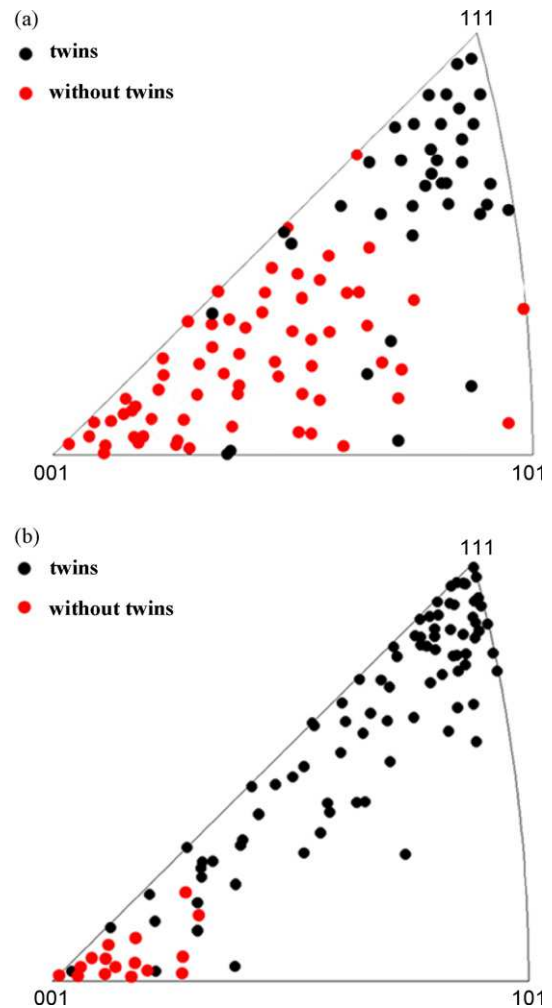


Fig. 6. Inverse pole figures along the tensile axis direction of steel LG (average grain size 50 μm) tensile strained to 0.05 logarithmic strain (a) and 0.3 logarithmic strain (b), respectively, showing grain orientations containing deformation twins (black dots) and without deformation twins (red dots). (For interpretation of the references to color in this figure legend, the reader is referred to the web version of the article.)

duces a strong decrease in the twin area fraction, from 0.2 for an average grain size of 50 μm to 0.1 for an average grain size of 3 μm at 0.3 logarithmic strain, but deformation twinning is still regularly observed in fine grains. As deformation twins are responsible for the outstanding mechanical properties of TWIP steels, this indicates that it is feasible to tailor the mechanical properties of Fe–22 wt.% Mn–0.6 wt.% C TWIP steels with grain refinement within the micrometer range. This is an interesting result regarding the optimization of the mechanical properties of TWIP steels. However, this result can at this stage not be generalized to other TWIP steel systems. For instance, Ueji et al. [5] reported a strong reduction in twinning activity in a Fe–31 wt.% Mn–3.0 wt.% Al–3.0 wt.% Si TWIP steel after similar grain refinement (average grain size of 1.8 μm) using also similar deformation conditions. The only difference is that the stacking fault energy (SFE) in Fe–31 wt.% Mn–3.0 wt.% Al–3.0 wt.% Si TWIP steel is larger than in the present Fe–22 wt.% Mn–0.6 wt.% C TWIP steel (around 40 mJ/m^2 against 22 mJ/m^2 [4,15]). These results indicate that the stacking fault energy, determined by chemical composition, plays a key role for the twinning behaviour in TWIP steels. Therefore, for a better understanding of twinning in TWIP steels both parameters, i.e. stacking fault energy and grain size, must be considered.

The influence of SFE on twinning is commonly considered as follows: Dislocation based models for deformation twinning in fcc

metals [10–13] propose that twinning is controlled by the glide of Shockley partials with Burgers vector $1/6 \langle 112 \rangle$ on $\{111\}$ planes. The critical resolved shear stress, τ_{critical} , to separate the leading Shockley partial from its trailing counterpart and thus create a twin is determined by a balance between the repulsive forces among the two Shockley partials and the attractive force of the SFE, given by

$$\tau_{\text{critical}} = \frac{\gamma}{b} \quad (1)$$

where γ is the SFE and b is the Burgers vector. As mentioned before, these models assume that twin nuclei already exist and therefore, only the stress for twin growth is estimated. Further, these models neither take into account the sources of dislocations nor a possible pile-up of dislocations in or at boundaries, thus the proposed twinning stress, τ_{critical} , can be considered as the twinning stress for a single crystal. The effect of grain size on deformation twinning still remains unclear. However, two approaches have been proposed to include the effect of grain size on twinning stress. In one approach [25] a Hall–Petch-type relation is proposed:

$$\tau_{\text{tw}} = \tau_0 + \frac{K_{\text{tw}}^{\text{H-P}}}{\sqrt{D}} \quad (2)$$

where τ_0 is the twinning stress for a single crystal, i.e. $\tau_0 = \tau_{\text{tw}} (D = \infty)$, and $K_{\text{tw}}^{\text{H-P}}$ is the Hall–Petch constant for twinning and D is the grain size. As explained above τ_0 can be replaced by γ/b leading to

$$\tau_{\text{tw}} = \frac{\gamma}{b} + \frac{K_{\text{tw}}^{\text{H-P}}}{\sqrt{D}} \quad (3)$$

This is a phenomenological relation which applies in many metals with different crystallographic structures such as hexagonal, bcc and fcc. Further, it has been reported that the Hall–Petch constant for twinning $K_{\text{tw}}^{\text{H-P}}$ is higher than that for slip $K_{\text{slip}}^{\text{H-P}}$ (for instance 10 times higher in Zr [26] and 2 times in copper [27]), although the reason for this difference is not well understood [25]. The other approach [28] proposes that the shear stress required to activate a twinning dislocation source is given by the shear stress to activate a Frank–Read source, $\tau_{\text{F-R}}$:

$$\tau_{\text{F-R}} = \frac{Gb}{2R} \quad (4)$$

where G is the shear modulus, b the Burgers vector and R the radius of the dislocation source. As twins are mainly nucleated at grain boundaries and the size of the softest possible dislocation source is proportional to the grain size, the following relation for the critical resolved shear stress for twinning is proposed:

$$\tau_{\text{tw}} = \frac{Gb}{D} \quad (5)$$

where G is the shear modulus, b is the Burgers vector and D is the grain size. This equation only describes the stress for nucleation of twins on boundaries. The growth of a twin in a homogeneous, single crystal matrix, however, is not considered. This growth stress is in principle the stress to drive the partial dislocations away from each other and may therefore be given by γ/b [10–13]. As a first approximation it should be independent of the grain size and can therefore be added to the nucleation stress, resulting in

$$\tau_{\text{tw}} = \frac{\gamma}{b} + \frac{Gb}{D} \quad (6)$$

In more detail, the grain size should have an effect, however, as grain size influences the yield stress which influences the hydrostatic pressure, which finally influences the stacking fault formation.

The examination of tensile strained samples by means of the ECCI technique reveals that deformation twinning occurs in both TWIP steels (steel LG and steel FG) at around 0.03 logarithmic strain.

This observation indicates that in the present TWIP steel deformation twinning initiates already at very low plastic strain, close to yielding. This result is consistent with previous observations by TEM in the same TWIP steel tensile deformed at room temperature where deformation twins were observed at 0.02 logarithmic strain [24]. Further studies on deformation twinning in fcc metals have also reported that deformation twinning is observed at small plastic strains [9,24,29]. However, the logarithmic stress at which deformation twinning was already activated (experimental twin stress) was higher in steel FG than in steel LG (steel FG: 400 MPa, steel LG: 270 MPa). This result indicates a clear effect of grain size on twin stress. However, this influence is not direct but indirect via slip, i.e. grain size mainly has an effect on slip. In fcc metals it has been observed that multiple slip is required for twinning, i.e. slip precedes twinning [9,12,29]. As explained above, in the present TWIP steel once multiple slip is activated deformation twinning occurs directly. These observations indicate a strong correlation between slip and twinning. As slip is influenced by the grain size via Hall–Petch a Hall–Petch-type dependence in twinning can therefore be expected. Table 1 shows the twinning stresses calculated from relations (3) and (6) for the present Fe–22 wt.% Mn–0.6 wt.% C TWIP steel. These stresses were calculated according to $\sigma_{\text{tw}} = \tau_{\text{tw}}/m$ assuming an average Schmid factor m of 0.326 [30], $\gamma = 22 \text{ mJ/m}^2$ [15], $b = 2.5 \times 10^{-10} \text{ m}$ [6], $G = 65 \text{ GPa}$ [6] and $K_{\text{tw}}^{\text{H-P}} = 356 \text{ MPa } \mu\text{m}^{1/2}$ [31]. As $K_{\text{tw}}^{\text{H-P}}$ is unknown $K_{\text{slip}}^{\text{H-P}}$ was used instead. Experimental twinning stresses are shown in the last column of Table 1. It can be seen that relation (3) overestimates the twinning stress but the grain size effect is properly reflected. Relation (6) estimates with high accuracy the twinning stress for an average grain size of 50 μm but provides a weak grain size dependence, which is not in agreement with experimental observations. These results suggest that in the micrometer range of the grain sizes studied in this work a Hall–Petch relation provides a good estimation of the influence of the grain size on the twinning stress.

It should be pointed out that the twinning stresses shown in Table 1 are calculated assuming $K_{\text{tw}}^{\text{H-P}} \sim K_{\text{slip}}^{\text{H-P}}$. Remarkably, this assumption provides reasonable twinning stresses suggesting that in the present TWIP steel $K_{\text{tw}}^{\text{H-P}} \leq K_{\text{slip}}^{\text{H-P}}$. This is a surprising result as there are very few studies reporting such behaviour [25]. Two significant conclusions can be obtained from this finding: (i) the effect of grain size on twinning stress is similar than on yield stress. Dislocation based models [10–13] propose that in fcc metals some specific dislocation reactions are needed to form a twin nucleus that subsequently evolves into a twin. It is also reported that in order to form such dislocation reactions multiple slip must be activated [9,12,29]. The experimental observation that deformation twinning occurs at small plastic strain close to yielding indicates that once multiple slip is activated deformation twinning occurs directly. $K_{\text{slip}}^{\text{H-P}}$ provides the resistance to slip propagation associated with the grain boundaries. The relation $K_{\text{tw}}^{\text{H-P}} \leq K_{\text{slip}}^{\text{H-P}}$ therefore indicates that the effect of grain size within the micrometer range on the twinning stress is mainly ascribed to the resistance to slip propagation associated to grain boundaries and, hence, to activate multiple slip inside the grains required to promote deformation twinning. (ii) For the present Fe–22 wt.% Mn–0.6 wt.% C TWIP steel, the effect of grain refinement within the micrometer range on the twinning stress and, hence, on twinning inhibition, is smaller than in other TWIP steels. This is supported by the experimental observation that in the present TWIP steel grain refinement within the micrometer range does not suppress twinning.

The relation (3) allows us to analyze separately the contribution of the stacking fault energy and grain size to the twinning stress. Fig. 7 shows the influence of both contributions, SFE and grain size, to the twinning stress of steel LG (average grain size of 50 μm) and steel FG (average grain size of 3 μm). It is seen that in both steels

Table 1

Estimated and experimental twinning stresses in a tensile deformed Fe–22 wt.% Mn–0.6 wt.% C TWIP steel with different average grain sizes.

Average grain size (μm)	$\sigma_{\text{tw}} = (1/m)(\gamma/b) + (K_{\text{tw}}^{\text{H-P}}/\sqrt{D})$ (MPa)	$\sigma_{\text{tw}} = (1/m)(\gamma/b) + (Gb/D)$ (MPa)	Experimental σ_{tw} (MPa)
50	323	274	270
3	478	290	400

the contribution of SFE to the twinning stress is larger than that of the grain size. For large grain sizes (above $50 \mu\text{m}$) the contribution of grain size to the twinning stress is small (50 MPa, less than 15% of the twinning stress), increasing its importance with grain size refinement. For an average grain size of $3 \mu\text{m}$ (steel FG) the contribution of grain size to twinning stress is similar to that of the SFE.

4.2. Effect of grain orientation

The main result concerning the influence of grain orientation on twinning behavior in the present TWIP steel tensile deformed at room temperature is that the grain orientation has a strong influence on deformation twinning at low strains but at high strains the influence decreases significantly.

The influence of grain orientation on deformation twinning is commonly explained in terms of Schmid's law for slip twin dislocations [7,15–17,29]:

$$\tau_{\text{tw}} = \sigma \cos \phi \cos \lambda \quad (7)$$

where $m = \cos \phi \cos \lambda$ is the Schmid factor, σ is the macroscopic stress in MPa, ϕ is the angle between the twinning plane normal and the tensile axis, and λ is the angle between the twinning shear direction and the tensile axis. We assume that Schmid's law is valid in the present study as in previous studies on similar TWIP steels [15], with the difference, of course, that twinning is unidirectional only. It is further assumed that the critical resolved shear stresses for both slip and twinning are approximately equal. This is supported by the strong correlation observed between slip and twinning in fcc metals, i.e. multiple slip is seen to be required for twinning to occur [9,12,29], and the results obtained in the present work showing that once multiple slip is activated twinning occurs readily resulting in similar stresses for both slip and twinning. However, this assumption does not imply that twinning can occur before slip because it is a necessary but not sufficient condition. Therefore, once multiple slip is activated, twinning occurs when the twinning stress τ_{tw} is larger than the slip stress τ_s , i.e. for those grains where the highest Schmid factor for twinning m_{tw} is larger than the highest Schmid factor for slip m_s , this is

$$m_{\text{tw}} > m_s \quad (8)$$

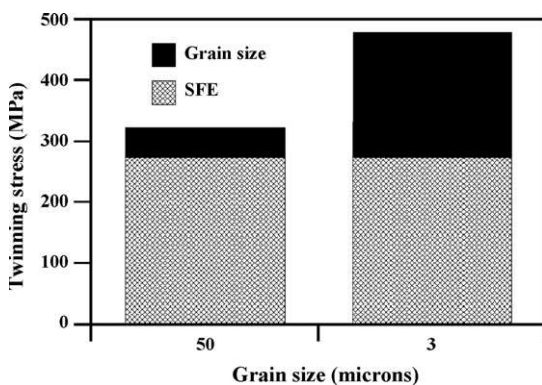


Fig. 7. Graph of the contribution of the stacking fault term (γ/b) and grain size term ($K_{\text{tw}}^{\text{H-P}}/\sqrt{D}$) on the twinning stress for steel LG (average grain $50 \mu\text{m}$) and steel FG (average grain $3 \mu\text{m}$).

Assuming this twinning criterion, the grain orientations favorable and unfavorable for twinning can be calculated for a particular macroscopic stress. Fig. 8(a) shows the TA-IPF with calculated grain orientations favorable (red lines) and unfavorable for twinning (blue lines) during tensile deformation. The figure reveals two regions of grain orientations where twinning is favorable or not. The predicted regions are in excellent agreement with the observed grain orientations in steel LG tensile deformed to 0.05 logarithmic strain, Fig. 8(b). Almost all observed orientations fall within the corresponding Schmid regime of the TA-IPF. This result indicates first that our assumption that the critical resolved shear stresses for slip and twinning are very similar is correct. Second, Schmid's law fully explains the strong influence of grain orientation on deformation twinning observed in steel LG tensile deformed to low strain. At this strain level deformation twinning mainly occurs in grains oriented close to the $\langle 111 \rangle$ /TA directions. Nevertheless, the Schmid law does not explain the small influence of the grain orientation on deformation twinning observed at higher

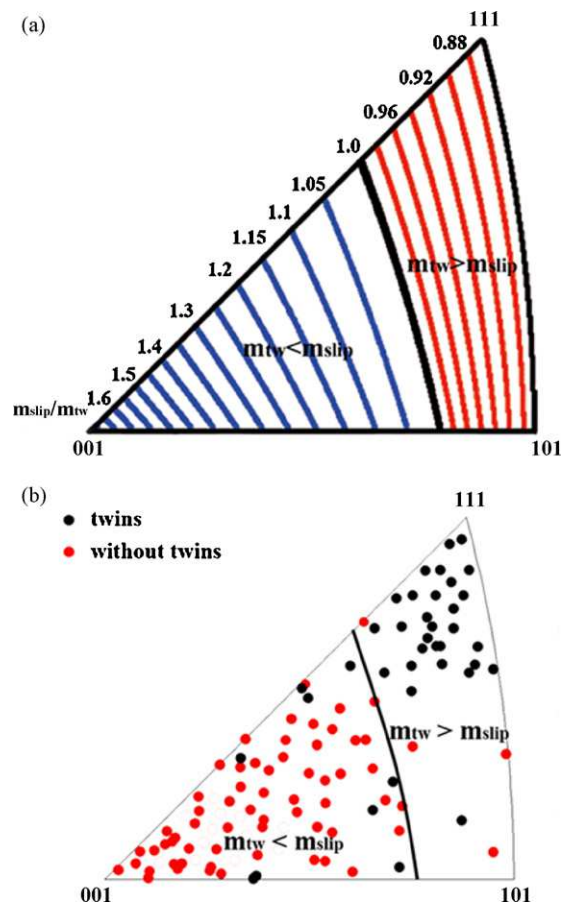


Fig. 8. (a) Inverse pole figure along tensile axis direction showing the grain orientations which are favorably (area with red lines) and unfavorably oriented (area with blue lines) for twinning according to the Schmid law and the assumption of equal critical resolved shear stresses for slip and twinning. (b) Comparison between experimental grain orientations (dots) obtained in steel LG (average grain size $50 \mu\text{m}$) tensile strained to 0.05 logarithmic strain and calculated orientation regions from the Schmid law. (For interpretation of the references to color in this figure legend, the reader is referred to the web version of the article.)

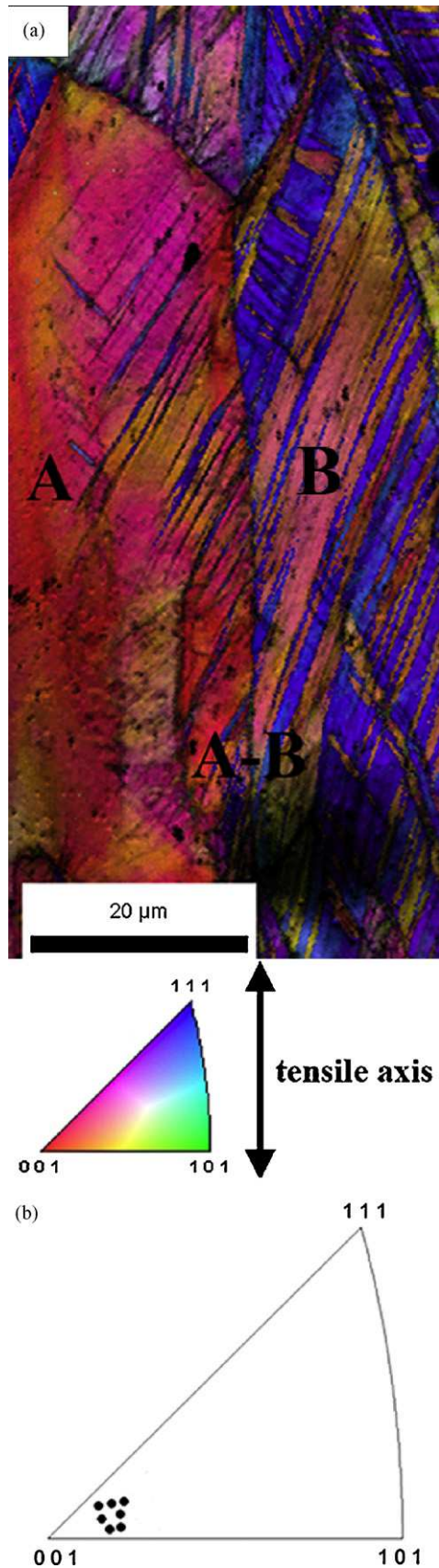


Fig. 9. (a) TA-IPF map of the steel LG (average grain size 50 μm) tensile deformed to 0.3 logarithmic strain showing a grain (grain A) that is unfavorably oriented for twinning with respect to the macroscopic stress which contains deformation twins; (b) TA-IPF of grain A (TA: tensile axis; IPF: inverse pole figure).

strain, as the TA-IPF in Fig. 6(b) shows. At 0.3 logarithmic strain, deformation twinning occurs regularly in grains oriented unfavorably for twinning according to Schmid's law taking into account the current grain orientation. Only grains oriented close to the $\langle 001 \rangle // TA$ directions are free of twins. The deviation from Schmid's law observed at high strain is not unexpected although surprisingly, it has not been reported in previous studies on TWIP steels [16,17]. This deviation can be explained as follows. The predicted orientations from Schmid's law, shown in the TA-IPF of Fig. 8(a), were calculated assuming the macroscopical unidirectional stress state to act in a similar manner everywhere in the material. In the present TWIP steel tensile deformed to high strain, the local stress state controlling deformation twinning may, however, be very different from the macroscopic one [21,32–34]. Figs. 1 and 2 reveal that the present TWIP steel develops during tensile deformation a complex and heterogeneous microstructure with a high amount of deformation twins. Deformation twins formed in one grain may create local shear stress concentrations at loci where they impinge on a grain boundary. This may lead to nucleation of twins in neighbouring grains even if they are – with respect to the macroscopic stress state – unfavourably oriented for twinning. The TA-IPF map in Fig. 9(a) shows an example of a grain unfavorably oriented for twinning with respect to the macroscopic stress which contains deformation twins (grain orientation spread is shown in the TA-IPF of Fig. 9(b)). The grain oriented close to the $\langle 001 \rangle // TA$ direction, referred to as grain A, is highly unfavorably oriented for twinning. Nevertheless, it contains a large amount of deformation twins which have, however, not grown all the way through the grain. These twins are nucleated at the grain boundary A-B where bundles of twins of the adjacent grain (grain B) impinged. A more detailed analysis on the twinning transfer across the grain boundaries would require consideration of the grain boundary character [22,34]. This has, however, not been done here.

5. Conclusions

We investigate the influence of grain size and grain orientation on deformation twinning in a tensile deformed Fe–22 wt.% Mn–0.6 wt.% C TWIP steel at room temperature. The following conclusions are drawn:

- Grain refinement within the micrometer range does not suppress deformation twinning. As deformation twins are responsible for the outstanding mechanical properties of TWIP steels, this indicates that it is feasible to tailor the mechanical properties of Fe–22 wt.% Mn–0.6 wt.% C TWIP steels with grain refinement within the micrometer range. As twinning stress is strongly dependent on the stacking fault energy, this result can not be extended to other TWIP steels as minor modifications in chemical composition may alter the stacking fault energy.
- A Hall–Petch relation $\sigma_{tw} = (\gamma/mb) + (K_{tw}^{H-P}/\sqrt{D})$ provides a good estimate of the effect of grain size within the micrometer range on the twinning stress. It was found that the Hall–Petch constant for twinning, K_{tw}^{H-P} , is about equal to that for slip, K_{slip}^{H-P} . Two significant conclusions can be drawn from this finding: (i) the effect of the grain size on twinning stress is similar to its effect on yield stress. This is ascribed to the resistance to slip propagation associated to grain boundaries. Slip propagation is associated to activation of multiple slip which is a prerequisite to deformation twin nucleation. (ii) For the present TWIP steel, the effect of grain refinement within the micrometer range on the twinning stress and, hence, on twinning inhibition, is smaller than in other TWIP steels.
- The orientation dependence of twinning at small strain shows that the critical resolved shear stress for twinning and slip are very similar as the appearance of twinning fully complies with

the Schmid law under these conditions. Deformation twinning mainly occurs in grains oriented close to $\langle 111 \rangle$ //tensile axis where the maximum resolved shear for twinning, τ_{tw} , is larger than that for slip, τ_s .

- At high strains (above 0.3 logarithmic strain), a strong deviation from the macroscopic Schmid law is observed. Deformation twins are observed in grains that are unfavourably oriented with respect to twinning according to Schmid's law. Local stress concentrations due to the accumulation of shear stresses at grain boundaries coming from incoming bundles of deformation twins, and also probably the grain boundary character, play an important role on the twinning behavior. This may lead to nucleation of twins in neighbouring grains even if they are – with respect to the macroscopic stress state – unfavourably oriented for twinning.

Acknowledgments

The authors would like to acknowledge the financial support by the German Research Foundation within the framework of the SFB 761 “steel ab initio”. The authors also acknowledge the help from Luc Hantcherli in the preparation of Fig. 8(a).

References

- [1] O. Grässel, L. Krüger, G. Frommeyer, L.W. Meyer, *Int. J. Plast.* 16 (2000) 1391–1409.
- [2] G. Frommeyer, U. Brück, P. Neumann, *ISIJ Int.* 43 (2003) 438–446.
- [3] S. Allain, J.P. Chateau, O. Bouaziz, *Mater. Sci. Eng. A* 387–389 (2004) 143–147.
- [4] S. Vercammen, B. Blanpain, B.C. De Cooman, P. Wollants, *Acta Mater.* 52 (2004) 2005–2012.
- [5] R. Ueji, N. Tsuchida, D. Terada, N. Tsuji, Y. Tanaka, A. Takemura, K. Kunishige, *Scr. Mater.* 59 (2008) 963–966.
- [6] O. Bouaziz, S. Allain, C. Scott, *Scr. Mater.* 58 (2008) 484–487.
- [7] M.N. Shiekhelsouk, V. Favier, K. Inal, M. Cherkaoui, *Int. J. Plast.* 25 (2009) 105–133.
- [8] T. Shun, C.M. Wan, J.G. Byrne, *Acta Metall. Mater.* 40 (1992) 3407–3412.
- [9] J.W. Christian, S. Mahajan, *Prog. Mater. Sci.* 39 (1995) 1–157.
- [10] J.A. Venables, *Phil. Mag.* 6 (1961) 379–396.
- [11] H. Fujita, T. Mori, *Scr. Metall.* 9 (1975) 631–636.
- [12] S. Mahajan, G.Y. Chin, *Acta Metall.* 21 (1973) 1353–1363.
- [13] N. Narita, J. Takamura, *Phil. Mag.* 29 (1974) 1001–1028.
- [14] T.H. Lee, C.S. Oh, S.J. Kim, S. Takaki, *Acta Mater.* 55 (2007) 3649–3662.
- [15] L. Bracke, L. Kestens, J. Penning, *Scr. Mater.* 61 (2009) 220–222.
- [16] P. Yang, Q. Xie, L. Meng, H. Ding, Z. Tang, *Scr. Mater.* 55 (2006) 629–631.
- [17] L. Meng, P. Yang, Q. Xie, H. Ding, Z. Tang, *Scr. Mater.* 56 (2007) 931–934.
- [18] D. Senk, H. Emmerich, J. Rezende, R. Siquieri, *Adv. Eng. Mater.* 9 (2007) 695–702.
- [19] C. Sachs, H. Fabritius, D. Raabe, *J. Struct. Biol.* 155 (2006) 409–425.
- [20] D. Raabe, M. Sachtleber, Z. Zhao, F. Roters, S. Zaefferer, *Acta Mater.* 49 (2001) 3433–3441.
- [21] D. Raabe, M. Sachtleber, H. Weiland, G. Scheele, Z. Zhao, *Acta Mater.* 51 (2003) 1539–1560.
- [22] S. Zaefferer, J.C. Kuo, Z. Zhao, M. Winning, D. Raabe, *Acta Mater.* 51 (2003) 4719–4735.
- [23] I. Gutierrez-Urrutia, S. Zaefferer, D. Raabe, *Scr. Mater.* 61 (2009) 737–740.
- [24] D. Barbier, N. Gey, S. Allain, N. Bozzolo, M. Humbert, *Mater. Sci. Eng. A* 500 (2009) 196–206.
- [25] M.A. Meyers, O. Vöhringer, V.A. Lubarda, *Acta Mater.* 49 (2001) 4025–4039.
- [26] S.G. Song, G.T. Gray III, *Metall. Mater. Trans.* 26A (1995) 2665–2675.
- [27] O. Vöhringer, *Z. Metallkd.* 67 (1976) 51.
- [28] W.Z. Han, Z.F. Zhang, S.D. Wu, S.X. Li, *Phil. Mag.* 88 (2008) 3011–3029.
- [29] I. Karaman, H. Sehitoglu, K. Gall, Y.I. Chumlyakov, H.J. Maier, *Acta Mater.* 48 (2000) 1345–1359.
- [30] G.I. Taylor, *J. Inst. Met.* 62 (1938) 307–324.
- [31] F. de las Cuevas, M. Reis, A. Ferraiuolo, G. Prato Longo, L.P. Karjalainen, J. Alkorta, J. Gil Sevillano, *Key Eng. Mater.* 423 (2010) 147–152.
- [32] Z. Zhao, M. Ramesh, D. Raabe, A. Cuitino, R. Radovitzky, *Int. J. Plast.* 24 (2008) 2278–2297.
- [33] M. Sachtleber, Z. Zhao, D. Raabe, *Mater. Sci. Eng. A* 336 (2002) 81–87.
- [34] T.R. Bieler, P. Eisenlohr, F. Roters, D. Kumar, D.E. Mason, M.A. Crimp, D. Raabe, *Int. J. Plast.* 25 (2009) 1655–1683.